

Synthesis and Characterization of New Organosilyl Derivatives of Polyoxometalates $(n\text{Bu}_4\text{N})_2[\text{NbW}_5\text{O}_{19}\text{SiRR}'_2]$ ($\text{R} = \text{R}' = \text{Et}$, $i\text{Pr}$, $Ot\text{Bu}$, Ph ; $\text{R} = t\text{Bu}$ and $\text{R}' = \text{Me}$) – X-ray Crystal Structure of $(n\text{Bu}_4\text{N})_2[\text{NbW}_5\text{O}_{19}\text{SiPh}_3]$

Fatma Bannani,^[a,b] René Thouvenot,^{*[b]} and Mongi Debbabi^{*[a]}

Keywords: Polyoxometalates / Organic–inorganic hybrid / Multinuclear NMR spectroscopy

Reactions of $(n\text{Bu}_4\text{N})_4[(\text{NbW}_5\text{O}_{18})_2\text{O}]$ with trialkyl/arylsilanols in dichloromethane and/or acetonitrile forms respectively $(n\text{Bu}_4\text{N})_2[\text{NbW}_5\text{O}_{19}\text{SiRR}'_2]$ [$\text{R} = \text{R}' = \text{Et}$ (**1**), $i\text{Pr}$ (**3**), $Ot\text{Bu}$ (**4**), Ph (**5**); $\text{R} = t\text{Bu}$ and $\text{R}' = \text{Me}$ (**2**)] in ca. 90–64 % isolated yields. The compounds have been characterized by elemental analysis, IR, Raman, multinuclear NMR in solution (^1H , ^{13}C , ^{29}Si , ^{183}W) and in the solid-state by ^{29}Si CP-MAS NMR spectroscopy. Multinuclear NMR and IR spectroscopic data suggest that the SiRR'_2^+ electrophilic fragment binds selectively to the terminal NbO oxygen atom which appears the most

reactive site in $(n\text{Bu}_4\text{N})_3[\text{NbW}_5\text{O}_{19}]$. This is supported by X-ray crystallographic analysis of $(n\text{Bu}_4\text{N})_2[\text{NbW}_5\text{O}_{19}\text{SiPh}_3]$ (**5**) which crystallizes in the monoclinic system, space group $P2_1/a$ with lattice parameters $a = 19.884(5)$, $b = 16.801(2)$, $c = 20.644(3)$ Å, $\beta = 112.050(12)^\circ$, $V = 6392(2)$ Å³, and $Z = 4$. Hydrolysis of the alkyl/arylsilyloxy derivatives leads to the back formation of the $(\text{NbW}_5\text{O}_{18})_2\text{O}^{4-}$ dimer by the cleavage of the Si–O bond.
(© Wiley-VCH Verlag GmbH & Co. KGaA, 69451 Weinheim, Germany, 2007)

Introduction

Polyoxometalates (POMs) form a class of inorganic metal-oxygen cluster compounds having a rising popularity in diverse fields ranging from catalysis to pharmacology.^[1] These interesting properties have increased studies to modify polyoxometalates and prepare new compounds in order to well understand polyoxometalates reactivities.^[2,3] One of the classical methods to obtain derivatized polyoxometalates is the reaction between the nucleophilic oxygen atom in d^0 transition metal oxocomplexes and electrophilic species^[4–6] such as organic and organometallic groups. With organic groups bearing reactive moieties, these hybrid species may be further functionalized to be ultimately grafted onto surfaces for obtaining photo- or electrochemical materials. While monosubstituted niobotungstates are relatively poorly reactive,^[7] dimeric species with connecting Nb–O–Nb bridge(s) are excellent starting materials for the preparation of organic and organometallic derivatized polyoxoanions.^[8–11] Herein, we report the preparation and char-

acterization by IR, Raman, and multinuclear NMR spectroscopy of the $n\text{Bu}_4\text{N}^+$ (TBA) salts of alkyl/arylsilylated Nb^{V} -monosubstituted Lindqvist POMs and the X-ray structural determination of $(n\text{Bu}_4\text{N})_2[\text{NbW}_5\text{O}_{19}\text{SiPh}_3]$ (**5**). In addition the reaction of these anions with respect to hydrolysis has been investigated.

Results and Discussion

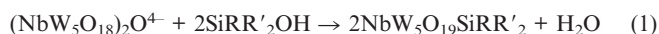
Synthesis and Reactivity

The substitution of Nb^{V} for W^{VI} in the inert hexatungstate results in the increase of the overall charge of the polyoxometalate and in partial localization of the supplementary charge on the terminal oxygen atoms bound to the Nb atom.^[17,18] Moreover, the oxygen–niobium bond in $\text{NbW}_5\text{O}_{19}$ is known to be labile with respect to ^{17}O exchange.^[8,19] Although the terminal ONb oxygen atoms are not the most basic among the oxygen atoms bound to Nb atoms both the lability and steric interaction allow reactions with electrophilic species to occur selectively at this oxygen site.^[8] Actually in the case of the substituted Keggin anion $\text{PW}_{11}\text{NbO}_{40}$ the reaction of $\text{Me}_3\text{SiSO}_3\text{CF}_3$ leads directly to the trimethylsilyl derivatives $\text{PW}_{11}\text{O}_{39}\text{NbOSiMe}_3$.^[20] In our case the reaction of $\text{R}_3\text{SiSO}_3\text{CF}_3$ ($\text{R} = \text{Me}$, Et) and $t\text{BuMe}_2\text{SiSO}_3\text{CF}_3$ with $\text{NbW}_5\text{O}_{19}^{3-}$ leads invariably to complex mixtures. By reacting alcohols and silanols with the dimeric form $(\text{Nb}_2\text{W}_4\text{O}_{18})_2\text{O}^{6-}$ instead of the monomer Klemperer described the clean synthesis of

[a] Laboratoire de Physico-Chimie des Matériaux, Faculté des Sciences de Monastir, 5019 Monastir, Tunisie
Fax: +216-73-500-514
E-mail: mongi.debbabi@enim.rnu.tn

[b] Laboratoire de Chimie Inorganique et Matériaux Moléculaires, UMR CNRS 7071, Université Pierre et Marie Curie – Paris 6, Institut de Chimie Moléculaire FR 2769, Case Courrier 42, 4, Place Jussieu, 75252 Paris Cedex 05, France
Fax: +33-1-44-27-38-41
E-mail: rth@ccr.jussieu.fr

terminal alkoxide and organosilyl-Lindqvist derivatives.^[21] Later Beer^[8] applied the same strategy to prepare terminal alkoxide Lindqvist derivatives by reacting the dimeric form of $\text{NbW}_5\text{O}_{19}^{3-}$ with alcohols. In light of the reactivities of the dimers it was expected that $(\text{NbW}_5\text{O}_{18})_2\text{O}^{4-}$ could also react under controlled conditions with silanols to give $\text{NbW}_5\text{O}_{19}\text{SiRR}'_2{}^{2-}$ according to Equation (1).



The reaction of $(n\text{Bu}_4\text{N})_4[(\text{NbW}_5\text{O}_{18})_2\text{O}]$ with a stoichiometric amount of $\text{RR}'_2\text{SiOH}$ at room temperature, under argon, in freshly distilled dichloromethane ($\text{R} = \text{R}' = \text{Et}$, $i\text{Pr}$; $\text{R} = t\text{Bu}$, $\text{R}' = \text{Me}$) or in acetonitrile ($\text{R} = \text{R}' = \text{Ph}$, $Ot\text{Bu}$) yields $\text{NbW}_5\text{O}_{19}\text{SiRR}'_2{}^{2-}$ [$\text{R} = \text{R}' = \text{Et}$ (1), $i\text{Pr}$ (3); $\text{R} = t\text{Bu}$, $\text{R}' = \text{Me}$ (2)] in satisfactory yields. For $\text{R} = \text{Ph}$ (5) or $Ot\text{Bu}$ (4) the low yields (ca. 25%) in CH_2Cl_2 were increased by using acetonitrile as the solvent.

As shown by the solution studies the hybrid anions are relatively stable in CH_2Cl_2 and CH_3CN but they are progressively hydrolyzed by atmospheric moisture to give $(\text{NbW}_5\text{O}_{18})_2\text{O}^{4-}$ which crystallizes from these solutions.

The formation of the dimer is described by Equation (2); the dimeric anion is in equilibrium with the protonated monomer according to Equation (3).



This behavior is similar to that observed by Klemperer on $(\text{Nb}_2\text{W}_4\text{O}_{18})_2\text{O}^{6-}$ and by Beer on $\alpha\text{-}\{\text{PW}_{11}\text{O}_{39}\}\text{-NbOEMe}_3$ ^{3-[20,21]} where ($\text{E} = \text{C}$, Si). Beer demonstrated using ^{17}O NMR that the primary hydrolysis product of the hybrid species is the dimer $(\alpha\text{-}\{\text{PNbW}_{11}\text{O}_{39}\})_2\text{O}^{6-}$ which hydrolyzes further to the monomer $\alpha\text{-PNbW}_{11}\text{O}_{40}^{4-}$.

In our case the reaction stops at the dimer because of its insolubility in dichloromethane and in acetonitrile.

Moreover, in more polar solvents such as DMSO the species are not stable and completely decompose into nonidentified species as shown by both IR and ^{183}W NMR spectroscopy.

Vibrational Spectroscopy

IR Characterization

Infrared spectroscopy analysis gives preliminary structural information in the solid state. Characteristic bands of the parent anion are present at nearly the same positions as in $(n\text{Bu}_4\text{N})_3[\text{NbW}_5\text{O}_{19}]$ namely at 810 cm^{-1} ($\nu_{\text{as}} \text{M-O}_b$), 584 cm^{-1} ($\nu_s \text{M-O}_b$), 446 cm^{-1} ($\delta \text{M-O}_b$) indicating that the Lindqvist structure is kept in the organic-inorganic hybrid. Nevertheless the strong band assigned to ($\nu_{\text{as}} \text{W-O}_t$) shifts from 958 cm^{-1} in $\text{NbW}_5\text{O}_{19}^{3-}$ to 971 cm^{-1} in $(\text{NbW}_5\text{O}_{18})_2\text{O}^{4-}$ and the organosilyl species. Such a high frequency shift has already been observed for Keggin silyl derivatives^[22] as a consequence of the grafting of organosilyl moieties on the POM framework. In the low-wave number region (from 300 to 1000 cm^{-1}) characteristic of the metal oxygen framework vibration, all compounds exhibit nearly identical spectra (Figure 1). The absence of the bands at 692 cm^{-1} characteristic of the Nb-O-Nb bridge of the $(\text{NbW}_5\text{O}_{18})_2\text{O}^{4-}$ shows that the hybrid species is built up from the monomeric anion while the lack of the Nb-O_t (915 cm^{-1}) in the $\text{NbW}_5\text{O}_{19}^{3-}$ ^{3-[23]} pleads in favor of derivatization at this terminal ONb oxygen atom.

Raman Characterization

Raman spectra of the dimer and of all hybrid derivatives are very similar in the low-wavenumber part ($\tilde{\nu} < 1050\text{ cm}^{-1}$)

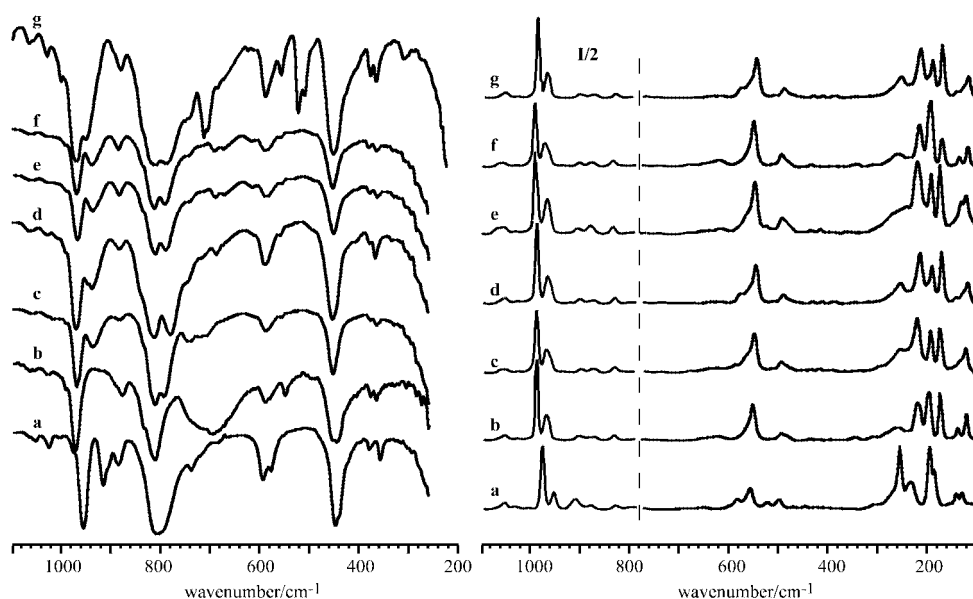


Figure 1. Infrared (left) and Raman (right) spectra of tetrabutylammonium salts of (a) $\text{NbW}_5\text{O}_{19}^{3-}$, (b) $(\text{NbW}_5\text{O}_{18})_2\text{O}^{4-}$, (c) $\text{NbW}_5\text{O}_{19}\text{SiEt}_3^{2-}$ (1), (d) $\text{NbW}_5\text{O}_{19}\text{Si}t\text{BuMe}_2^{2-}$ (2), (e) $\text{NbW}_5\text{O}_{19}\text{Si}i\text{Pr}_3^{2-}$ (3), (f) $\text{NbW}_5\text{O}_{19}\text{Si}(Ot\text{Bu})_3^{2-}$ (4), (g) $\text{NbW}_5\text{O}_{19}\text{SiPh}_3^{2-}$ (5). The high frequency part ($>800\text{ cm}^{-1}$) of the Raman spectra is scaled by half.

(Figure 1). They differ markedly from the spectrum of $\text{NbW}_5\text{O}_{19}^{3-}$ in the low frequency region $<300\text{ cm}^{-1}$ and also in the high frequency region ($900\text{--}1000\text{ cm}^{-1}$); in particular as for IR the $\nu_s(\text{W--O}_t)$ and $\nu_{as}(\text{W--O}_t)$ are shifted by ca. 13 cm^{-1} to a higher frequency in the dimer and in the hybrid species.

Multinuclear NMR Characterization

The presence of several NMR active nuclei allows the structural characterization of POMs by multinuclear NMR spectroscopy.^[24–28] Moreover, the high solubility of the TBA salt of POMs in some polar organic solvent permits us to prepare the concentrated solutions required for ^{183}W and ^{29}Si NMR spectroscopy. Multinuclear NMR (^1H , ^{13}C , ^{29}Si , and ^{183}W) measurements have been performed in dichloromethane and acetonitrile solutions. Because of the presence of the organic moieties, $\text{NbW}_5\text{O}_{19}\text{SiRR}'_2$ hybrids are soluble in the less polar organic solvents such as CH_2Cl_2 .

The ^1H and ^{13}C spectra of the hybrid species present the signals characteristic of the organosilyl part along with those of the TBA cations (see experimental part). The relative integration of the signals agrees with two TBA for one SiRR'_2 group according to the formula $(n\text{Bu}_4\text{N})_2\text{[NbW}_5\text{O}_{19}\text{SiRR}'_2]$.

Room-temperature solid-state ^{29}Si CP-MAS spectra were obtained for compounds **1**, **2**, **3**, and **5** (Table 1). They all present only one isotropic signal; while for **3** the signal is relatively narrow ($\Delta\nu_{1/2}$ ca. 100 Hz, 1.3 ppm), it appears broader for the three other compounds ($\Delta\nu_{1/2}$ 300 to 500 Hz, see Table 1); this differential behavior is likely due to more or less rapid rotation around the Si–O bond, leading to different motional narrowing of the ^{29}Si resonances. No significant signal could, however, be obtained for compound **4**, even with a large contact time, likely because of inefficient transfer between the silicium nucleus and the more remote protons. The ^{29}Si solution spectra present also a single line; contrary to the ^{29}Si spectra of the silyl derivatives of Keggin polyoxometallates,^[22,27] no ^{183}W satellites could be detected for the NbW_5 hybrids; this is again in favor of the SiRR'_2 group grafted on $\text{O}_t\text{--Nb}$. The observed chemical shifts are as expected for the M (SiOC_3) group in the case of **1**, **2**, **3**, and **5** and for a Q (SiO_4) group for **4** (see Table 1). The close values of the isotropic chemical shifts in solution and in the solid-state indicate that hybrid anions

keep their structures in solution; at variance with the solid-state case, the line in the solution spectra are, however, very narrow, which agrees with rapid reorientation of the organosilyl part in solution.

The ^{183}W NMR spectra of all compounds exhibit two narrow signals around 28–35 ppm (4 W) and 75–79 ppm (1 W) assigned to four equatorial and one axial tungsten atoms, respectively (Figure 2). Each signal presents a pair of satellites due to homonuclear tungsten–tungsten coupling with a coupling constant value (9 Hz) in the classical range characteristic of an “edge-sharing-junction” in iso- and heteropolyanions.^[24,26,28] This is again consistent with an effective C_{4v} symmetry of the hybrid anions in solution, with rapid reorientation of the organosilyl group grafted onto the terminal $\text{O}_t\text{--Nb}$ oxygen atom.

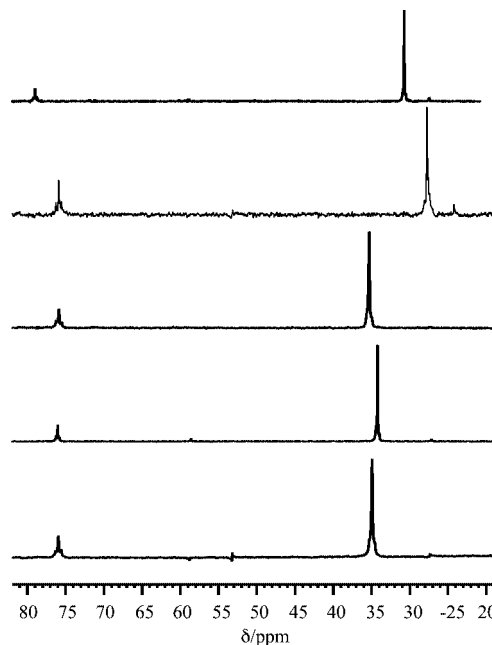


Figure 2. ^{183}W NMR solution spectra of the siloxide derivatives: from top to bottom, $\text{NbW}_5\text{O}_{19}\text{SiPh}_3^{2-}$ (**5**), $\text{NbW}_5\text{O}_{19}\text{Si}(\text{OtBu})_3^{2-}$ (**4**), $\text{NbW}_5\text{O}_{19}\text{SiPr}_3^{2-}$ (**3**), $\text{NbW}_5\text{O}_{19}\text{Si}(\text{BuMe}_2)^{2-}$ (**2**), and $\text{NbW}_5\text{O}_{19}\text{SiEt}_3^{2-}$ (**1**).

The ^{183}W chemical shifts are known to be extremely sensitive to subtle structural changes.

In the present case changing the substituent on the Si atom induces chemical shift variations of ca. 7 and 4 ppm

Table 1. ^{183}W and ^{29}Si NMR spectroscopic data for Nb^V -monosubstituted Lindqvist polyoxometalates.

Compound	^{183}W $\delta(W_{ax})^{[a]}$	$\Delta(W_{eq})^{[a]}$	$\Delta\delta^{[b]}$	^{29}Si $\delta^{[c]}$	$\delta_{iso}^{[d]}$	$\Delta\nu_{1/2}^{[e]}$
$\text{NbW}_5\text{O}_{19}\text{SiEt}_3^{2-}$ (1)	75.9	34.9	+41	25.8	26.8	400 (5)
$\text{NbW}_5\text{O}_{19}\text{Si}(\text{BuMe}_2)^{2-}$ (2)	76.3	34.5	+41.8	25.6	25.5	500 (6.3)
$\text{NbW}_5\text{O}_{19}\text{SiPr}_3^{2-}$ (3)	75.9	35.3	+40.5	24.8	22	100 (1.3)
$\text{NbW}_5\text{O}_{19}\text{Si}(\text{OtBu})_3^{2-}$ (4)	75.9	27.7	+48.2	−100.7		
$\text{NbW}_5\text{O}_{19}\text{SiPh}_3^{2-}$ (5)	79.0	30.7	+48.3	−15	−15.1	300 (3.7)
$(\text{NbW}_5\text{O}_{18})_2\text{O}^{4-}$	75.0	24.5	+50.5			
$\text{NbW}_5\text{O}_{19}^{3-}$	30.5	74.1	−43.6			

[a] δ values, ppm. [b] $\Delta\delta = \delta(W_{ax}) - \delta(W_{eq})$. [c] δ values, ppm; solution spectra. [d] δ values, ppm; solid-state CP-MAS spectra. [e] Full width at half maximum of the isotropic signal; in Hz and ppm (in brackets).

for equatorial and axial W nuclei, respectively. These small variations are nevertheless relatively important if we consider that these W atoms are five- and seven-bond remote from the substituting atom. Moreover, by comparison with the monomeric nonderivatized anion, the signals of the two types of W nuclei exchange their position and shift to the opposite direction in $(\text{NbW}_5\text{O}_{18})_2\text{O}^{4-}$ and in the silicon derivatives, i.e. the equatorial Ws are shielded by ca. 40 ppm in the organosilyl derivatives and by ca. 50 ppm in the dimer while the axial Ws are deshielded by about 45 ppm (Figure 3). This behavior has been already noticed by Finke on niobium derivatives of the Keggin anion: dimerization of SiNb_3W_9 by formation of three Nb–O–Nb bridges induces the shielding of the proximal W by ca. 30 ppm.^[9]

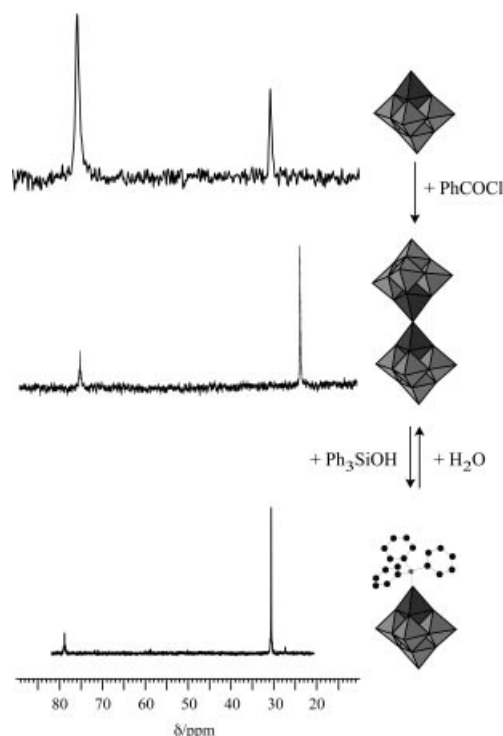


Figure 3. Comparison of the ^{183}W NMR spectra of: from top to bottom, $\text{NbW}_5\text{O}_{19}^{3-}$, $(\text{NbW}_5\text{O}_{18})_2\text{O}^{4-}$, and $\text{NbW}_5\text{O}_{19}\text{SiPh}_3^{2-}$ (left) and schematic representation of the formation and cleavage of $\text{NbW}_5\text{O}_{19}\text{SiPh}_3^{2-}$.

^{93}Nb NMR was registered for two compounds namely **2** and **4**; as was observed by Beer et al. for the dimeric form, the ^{93}Nb resonances of the silyl derivatives are very broad compared with that of underivatized monomeric $\text{NbW}_5\text{O}_{19}$. While the line width for a concentrated viscous solution of $\text{NbW}_5\text{O}_{19}^{3-}$ in DMSO does not exceed 5 kHz, it amounts to 12 and 25 kHz for **4** and **2** in diluted solution in the low-viscosity solvents acetonitrile and dichloromethane, respectively. This large ^{93}Nb line width originates from very rapid quadrupolar relaxation of the ^{93}Nb nucleus ($I = 9/2$); such a rapid relaxation ($T_2 < 3 \mu\text{s}$) explains the narrow ^{183}W resonance due to an effective self-decoupling of the ^{93}Nb nucleus.

X-ray Diffraction Analysis of $(n\text{Bu}_4\text{N})_2[\text{NbW}_5\text{O}_{19}\text{SiPh}_3]$ (**5**)

Whatever the nature of the solvents, attempts to grow crystals of hybrids suitable for X-ray crystallographic study were unsuccessful. Actually in all cases the crystals which formed were proved to contain the poorly soluble μ -oxo-bridged dimer $(\text{NbW}_5\text{O}_{18})_2\text{O}^{4-}$ which was formed by hydrolysis of the organosilyl $\text{NbW}_5\text{O}_{19}\text{SiR}_3^{2-}$ compounds (see above). Nevertheless, good quality crystals of $(n\text{Bu}_4\text{N})_2[\text{NbW}_5\text{O}_{19}\text{SiPh}_3]$ were formed slowly at room temperature on the bottom of the firmly taped NMR tube containing the concentrated acetonitrile solution. The molecular structure of the anion **5** is shown in Figure 4. The X-ray single crystal study confirmed the monomeric structure of **5**, in fact the structure of the hybrid anion is built up from the monosubstituted Lindqvist anion $\text{NbW}_5\text{O}_{19}$ on which is grafted the $\{\text{Si}(\text{C}_6\text{H}_5)_3\}$ fragment through the terminal O_7 –Nb oxygen atom. The asymmetric unit contains one $\text{NbW}_5\text{O}_{19}\text{SiPh}_3^{2-}$ anion and two TBA cations. The hybrid anion $\text{NbW}_5\text{O}_{19}\text{SiPh}_3^{2-}$ does not possess any crystallographic symmetry element in the solid state. However, in solution, because of rapid reorientation of the organosilyl fragment, the symmetry of the hybrid anion is consistent with C_{4v} as shown by ^{183}W NMR spectroscopy. Moreover, the grafting of this fragment to the Lindqvist anion hinders the random orientational disorder of the $\text{NbW}_5\text{O}_{19}$ unit^[12] and allows differentiation of the Nb from the W atoms and access to precise metrical data for these anions (Table 2).

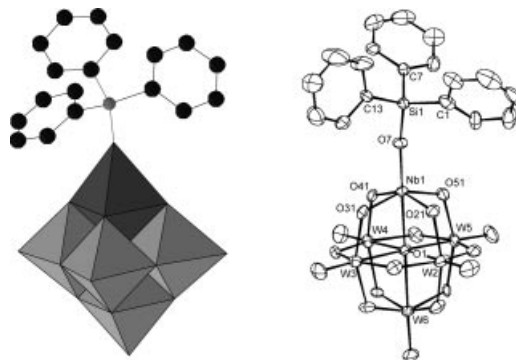


Figure 4. Representations of the molecular structure of $\text{NbW}_5\text{O}_{19}\text{SiPh}_3^{2-}$. Left: combined polyhedral and ball and stick model; right: Cameron representation with ellipsoids drawn at the 30% probability level.

The Nb–O bond length of 1.871(9) Å in the Nb–O–Si bridge compares well with similar bonds in $(n\text{Bu}_4\text{N})_3[\text{Nb}_2\text{W}_4\text{O}_{19}\{\text{Si}(\text{Me})_2(\text{CMe}_3)\}]$ [1.86(2) Å], while the Nb–O–Si bridge is more open (167°) in **5** than in the $\text{Nb}_2\text{W}_4\text{O}_{19}$ derivative (154°). The mean terminal and bridging W–O (1.70 and 1.92 Å, respectively) are also similar to those observed in $\text{W}_6\text{O}_{19}^{2-}$ (1.69 and 1.92 Å).^[29]

Concerning the metal–central oxygen distances, Nb–O₁ (2.262 Å) is significantly shorter than the W–O mean value for the equatorial bonds W–O₁ (2.32 Å) and than the axial W₆–O₁ (2.373 Å); the relatively short Nb–O_c distance is a consequence of the reduced *trans* influence of O₇ in the Nb–O–Si bridge. Analogous contractions have been observed in

Table 2. Selected bond lengths [Å] and angles [°] for $(n\text{Bu}_4\text{N})_2\text{[NbW}_5\text{O}_{19}\text{SiPh}_3\text{]} (5)$.

Nb1–O7	1.871(9)	Nb1–O21–W2	117.51(50)
Nb1–O1	2.262(9)	Nb1–O31–W3	116.09(46)
Nb1–O21	1.945(9)	Nb1–O41–W4	116.25(50)
Nb1–O31	1.968(12)	Nb1–O51–W5	117.33(45)
Nb1–O41	1.951(11)	Nb1–O7–Si1	167.15(56)
Nb1–O51	1.952(12)	O7–Si1–C1	110.58(51)
W2–O1	2.318(9)	O7–Si1–C7	108.48(51)
W3–O1	2.318(11)	O7–Si1–C13	106.51(64)
W4–O1	2.318(11)	C1–Si1–C7	111.22(75)
W5–O1	2.341(11)	C1–Si1–C13	111.76(81)
Si1–O7	1.638(9)	C7–Si1–C13	108.11(67)
Si1–C1	1.838(16)		
Si1–C7	1.871(17)		

monofunctionalized Lindqvist-type polyoxometallates such as $\text{Nb}_2\text{W}_4\text{O}_{19}\text{Si}(\text{Me})_2(\text{CMe}_3)^{3-}$ where Nb–O_c and W_{ax}–O_c amount to 2.27 and 2.37 Å, respectively. The remaining geometrical parameters of the NbW₅O₁₉ core are very similar; for example Nb–O–W bridge angles (between 116.09 and 117.51°) are only slightly smaller than the W–O–W ones (between 117.09 and 118.93°).

The tetrahedral Si atom displays a slight distortion from ideal geometry toward the terminal O–Nb bond with C–Si–C and O–Si–C angles on average 110.0° and 108.3°, respectively. The Si–C distances, which range from 1.823(19) to 1.871(19) Å, are longer than Si–O [1.633(11) Å].

Conclusions

In this work we report a valuable method for the clean preparation of organosilyl derivatives of monosubstituted hexaniobotungstate in good yields. Equation (1) features this functionalization which consists of a selective coordination of an electrophilic fragment $\{\text{SiRR}'_2\}^+$ [$\text{R} = \text{R}' = \text{Et}$ (**1**), $i\text{Pr}$ (**3**), $o\text{tBu}$ (**4**), Ph (**5**); $\text{R} = t\text{Bu}$ and $\text{R}' = \text{Me}$ (**2**)] to the terminal Nb–O_t oxygen atom which leads to the formation of a terminal organosilyloxy-derivatized monosubstituted niobotungstate. This organic–inorganic hybrid has a good solubility in a variety of polar organic solvents that makes it easily studied and characterized in solution by multinuclear NMR spectroscopy. Spectroscopic studies, along with an X-ray study of $\text{NbW}_5\text{O}_{19}\text{SiPh}_3^{2-}$ show that derivatization of $\text{NbW}_5\text{O}_{19}^{3-}$ occurs selectively at the terminal Nb–O_t rather than the bridging Nb–O_b–W oxygen atoms. Grafting of R_3Si^+ permits the resolution of the disorder problem in crystal structure. Hydrolysis of the siloxide derivative occurs at the Si–O bond and leads to the back formation of the starting material $(\text{NbW}_5\text{O}_{18})_2\text{O}^{4-}$.

Experimental Section

Reagents and Methods: Solvents (analytical grade) and the following reagents were purchased from commercial sources and used without further purification: triphenylsilanol, triethylsilanol, triisopropylsilanol, *tert*-butyldimethylsilanol, tri-*tert*-butoxysilanol, diethyl ether. Acetonitrile and dichloromethane were distilled under argon from CaH_2 . Syntheses of $(n\text{Bu}_4\text{N})_4[(\text{NbW}_5\text{O}_{18})_2\text{O}]$ and

$(n\text{Bu}_4\text{N})_3[\text{NbW}_5\text{O}_{19}]$ followed literature procedures described.^[8,12] All subsequent reactions were performed under an inert atmosphere of argon in a Schlenk line to avoid the polymerization of the silanols by the air moisture. The ^1H and ^{13}C spectra were obtained at 300 K from CD_2Cl_2 and CD_3CN solutions in 5-mm o.d. tubes at 300 and 75.5 MHz, respectively, with Bruker AC300 or Bruker AvanceII spectrometers. ^{29}Si and ^{183}W spectra were recorded at 300 K from $\text{CH}_2\text{Cl}_2/\text{CD}_2\text{Cl}_2$ solution in a 10-mm o.d. tube with the Bruker AC300 (59.6 and 12.5 MHz) and Bruker DRX 500 (99.3 and 20.8 MHz) spectrometers. Chemical shift values for ^1H , ^{13}C , and ^{29}Si were internally referenced to tetramethylsilane (TMS) using the solvent peak as secondary standard and for ^{183}W are given with respect to an external 2 M Na_2WO_4 solution in alkaline D_2O , using a saturated solution of dodecatungstosilicic acid ($\text{SiW}_{12}\text{O}_{40}\text{H}_4$) as a secondary standard ($\delta = -103.8$ ppm). The solid-state ^{29}Si NMR CP-MAS spectra were obtained at room temperature with a Bruker Avance 400 spectrometer operating at 79.5 MHz; spinning rates of 5 kHz, contact times of 3 to 10 ms, and a recycling delay of 5 s were used for obtaining spinning-sideband-free spectra in ca. 10 h. Chemical shifts of the isotropic line are reported with respect to TMS. FTIR spectra were recorded from KBr pellets with a Bio-rad FTS 165 IR-FT spectrometer with a resolution of 4 cm^{-1} . Raman spectra were collected with a Kaiser Optical Systems HL5R Raman spectrometer equipped with a near-IR laser diode working at 785 nm. The laser power was adjusted to 10–15 mW at the sample position for all spectra. The average resolution is equal to 3 cm^{-1} . Elemental analyses were performed by the Laboratoire Central d'Analyses du CNRS (Vernaison, France).

Crystal-Structure Analysis: Crystal structure data are summarized in Table 3. A colorless parallelepiped crystal ($0.08 \times 0.10 \times 0.25$ mm) of $(n\text{Bu}_4\text{N})_2[\text{NbW}_5\text{O}_{19}\text{SiPh}_3]$ was glued to a glass fiber, covered with a thin layer of epoxy cement, and examined by X-ray crystallography. Data were collected with a Kappa-CCD Bruker AXS diffractometer at 300 K using graphite-monochromated Mo-K_α radiation ($\lambda = 0.71073$ Å). Lattice parameters were obtained by

Table 3. Crystal data and structure refinement for $(n\text{Bu}_4\text{N})_2\text{[NbW}_5\text{O}_{19}\text{SiPh}_3] (5)$.^[a]

Empirical formula	$\text{C}_{50}\text{H}_{87}\text{N}_2\text{NbO}_{19}\text{SiW}_5$
Formula mass [g mol^{-1}]	3762.25
Crystal system	monoclinic
Space group	$P2_1/a$
a [Å]	19.884(5)
b [Å]	16.801(2)
c [Å]	20.644(3)
β [°]	112.050(12)
V [Å ³]	6329(2)
Z	4
μ [cm^{-1}]	9.219
$\rho_{\text{calcd.}}$ [g cm^{-3}]	2.141
θ range [°]	4–22
Index range	$-27 \leq h \leq 20$, $-23 \leq k \leq 22$, $-29 \leq l \leq 29$
Reflections collected	63469
Independent reflections	18157
Reflections with $I > 3\sigma(I)$	6674
Parameters refined	533
Goodness of fit, S	1.09
R	0.0434
R_w^*	0.0517
$\Delta\rho$ (max/min) [$\text{e}\cdot\text{\AA}^{-3}$]	2.54/–1.82

[a] Weighting scheme of the form $w = w' \{1 - [(|F_o| - |F_c|)/6\sigma(F_o)]^2\}^2$ with $w' = 1/\Sigma_w A_i T_i(X)$ with coefficients 2.56, 0.00658, 2.13 for a Chebyshev series for which $X = F_o/F_c(\text{max})$.

least-squares refinement of the diffraction data of 151 reflections within the range of $4^\circ < 2\theta < 22^\circ$. The index ranges of data collection were $-27 \leq h \leq 20$, $-23 \leq k \leq 22$, $-29 \leq l \leq 29$. Intensity data were collected using 6674 reflections with $I \geq 3\sigma(I)$. The structure was solved by direct methods and refined with full-matrix least-squares technique on F using the SHELXS86^[13] and CRYSTALS^[14] programs. Hybrid anion atom parameters were refined anisotropically and TBA cations were refined isotropically. The values of the discrepancy indices R_1 (R_w) for all data were 0.0434 (0.0517). The molecular structure was drawn with Diamond and Cameron programs^[15,16] and reported in Figure 4.

CCDC-635634 contains the supplementary crystallographic data for this paper. These data can be obtained free of charge from The Cambridge Crystallographic Data Centre via www.ccdc.cam.ac.uk/data_request/cif.

(*n*Bu₄N)₂[NbW₅O₁₉SiEt₃] (1): To a suspension of (*n*Bu₄N)₄[(NbW₅O₁₈)₂O] (1 g, 0.28 mmol) in 30 mL of dry dichloromethane was added (C₂H₅)₃SiOH (0.086 mL, 0.56 mmol). The resulting solution was stirred vigorously at ambient temperature under a static argon atmosphere for 24 h, then centrifuged at 4000 rpm for 15 min. The supernatant was added with diethyl ether, whilst stirring, precipitation of the hybrid has generally to be initiated by scraping the beaker walls with a glass spatula; the white precipitate was filtered and washed three times with 100 mL of diethyl ether and dried under vacuum to give 788 mg of crude product (73% yield). C₃₈H₈₇N₂NbO₁₉SiW₅ (1916.23): calcd. C 23.79, H 4.57, N 1.46, Nb 4.84, W 47.99; found C 23.73, H 4.57, N 1.33, Nb 4.16, W 47.35. IR (1300–400): $\tilde{\nu}$ = 446 (s), 583 (m), 706 (m), 718 (m), 742 (m), 792 (vs), 809 (vs), 884 (w), 938 (m), 971 (vs), 1239 (w) cm⁻¹. ¹H NMR (CD₂Cl₂): δ = 3.28 (t, 16 H, N-CH₂-CH₂-CH₂-CH₃), 1.71 (q, 16 H, N-CH₂-CH₂-CH₂-CH₃), 1.49 (m, 16 H, N-CH₂-CH₂-CH₂-CH₃), 1.08 (m, 33 H, N-CH₂-CH₂-CH₂-CH₃), 0.75 (q, 6 H, Si-CH₂-CH₃) ppm. ¹³C NMR (CD₂Cl₂): δ = 59.06 (N-CH₂-CH₂-CH₂-CH₃), 24.34 (N-CH₂-CH₂-CH₂-CH₃), 20.09 (N-CH₂-CH₂-CH₂-CH₃), 13.89 (N-CH₂-CH₂-CH₂-CH₃), 6.61 (Si-CH₂-CH₃), 7.47 (Si-CH₂-CH₃) ppm. ²⁹Si NMR (0.06 M, CH₂Cl₂/CD₂Cl₂): δ = 25.8 ppm. ¹⁸³W NMR (0.06 M, CH₂Cl₂/CD₂Cl₂): δ = 34.9 (J_{W-W} = 8.8 Hz, 4 W, W_{eq}), 75.9 (J_{W-W} = 8.8 Hz, 1 W, W_{ax}) ppm.

(*n*Bu₄N)₂[NbW₅O₁₉Si*i*BuMe₂] (2): This compound was prepared by the same procedure as for **1** using [C(CH₃)₃(CH₃)₂]SiOH (0.16 mL, 0.56 mmol) instead of (C₂H₅)₃SiOH (yield of crude product: 977 mg, 91%). C₃₈H₈₇N₂NbO₁₉SiW₅ (1916.23): calcd. C 23.79, H 4.57, N 1.46, Nb 4.84, W 47.99; found C 23.62, H 4.53, N 1.33, Nb 4.43, W 47.5. IR (1300–400): $\tilde{\nu}$ = 446 (s), 583 (m), 683 (w), 738 (sh), 777 (vs), 810 (vs), 881 (w), 938 (m), 970 (vs), 1029 (w), 1066 (w), 1108 (w), 1152 (w), 1253 (m) cm⁻¹. ¹H NMR (CD₂Cl₂): δ = 3.28 (t, 16 H, N-CH₂-CH₂-CH₂-CH₃), 1.72 (q, 16 H, N-CH₂-CH₂-CH₂-CH₃), 1.49 (m, 16 H, N-CH₂-CH₂-CH₂-CH₃), 1.08 (m, 33 H, N-CH₂-CH₂-CH₂-CH₃), 0.24 [s, 6 H, Si(CH₃)₂C(CH₃)₃] ppm. ¹³C NMR (CD₂Cl₂): δ = 58.57 (N-CH₂-CH₂-CH₂-CH₃), 25.31 [Si(CH₃)₂C(CH₃)₃], 23.98 (N-CH₂-CH₂-CH₂-CH₃), 19.67 (N-CH₂-CH₂-CH₂-CH₃), 19 [Si(CH₃)₂C(CH₃)₃], 13.54 (N-CH₂-CH₂-CH₂-CH₃), -3.85 [Si(CH₃)₂C(CH₃)₃] ppm. ²⁹Si NMR (0.06 M, CH₂Cl₂/CD₂Cl₂): δ = 25.7 ppm. ¹⁸³W NMR (0.06 M, CH₂Cl₂/CD₂Cl₂): δ = 34.5 (J_{W-W} = 8.8 Hz, 4 W, W_{eq}), 76.3 (J_{W-W} = 8.8 Hz, 1 W, W_{ax}) ppm.

(*n*Bu₄N)₂[NbW₅O₁₉Si*i*Pr₃] (3): This compound was prepared by the same procedure as for **1** using [CH(CH₃)₂]₃SiOH (0.11 mL, 0.56 mmol) instead of (C₂H₅)₃SiOH (yield of crude product: 923 mg, 84%). C₄₁H₉₃N₂NbO₁₉SiW₅ (1958.27): calcd. C 25.12, H 4.78, N 1.43, Si 1.43, W 46.96; found C 24.87, H 4.74, N 1.23, W 46.12. IR (1300–400): $\tilde{\nu}$ = 445 (vs), 583 (m), 611 (w), 668 (sh), 687

(w), 739 (sh), 788 (vs), 809 (vs), 883 (m), 969 (vs), 1062 (w), 1107 (w), 1152 (w), 1247 (w) cm⁻¹. ¹³C NMR (CD₂Cl₂): δ = 58.42 (N-CH₂-CH₂-CH₂-CH₃), 23.59 (N-CH₂-CH₂-CH₂-CH₃), 19.46 (N-CH₂-CH₂-CH₂-CH₃), 17.1 [SiCH(CH₃)₂], 13.06 (N-CH₂-CH₂-CH₂-CH₃), 0.81 [SiCH(CH₃)₂] ppm. ²⁹Si NMR (0.06 M, CH₂Cl₂/CD₂Cl₂): δ = 24.8 ppm. ¹⁸³W NMR (0.06 M, CH₂Cl₂/CD₂Cl₂): δ = 35.3 (J_{W-W} = 9 Hz, 4 W, W_{eq}), 75.9 (J_{W-W} = 9 Hz, 1 W, W_{ax}) ppm.

(*n*Bu₄N)₂[NbW₅O₁₉Si(*Or*Bu)₃] (4): To a suspension of (*n*Bu₄N)₄[(NbW₅O₁₈)₂O] (1 g, 0.28 mmol) in 30 mL of dry acetonitrile was added, under argon, [OC(CH₃)₃]₃SiOH (148 mg, 0.56 mmol). The resulting clear colorless solution was stirred vigorously at room temperature for 24 h. This solution was centrifuged at 4000 rpm for 15 min and then diethyl ether was added to the supernatant from which a white powder was precipitated under vigorous stirring. It was washed twice with diethyl ether and dried under vacuum to give 1013 mg in 88% yield. IR (1400–400): $\tilde{\nu}$ = 447 (s), 511 (w), 540 (w), 584 (m), 651 (m), 705 (m), 741 (m), 791 (vs), 811 (vs), 880 (m), 938 (m), 968 (vs), 996 (m), 1031 (m), 1077 (vs), 1189 (s), 1244 (s), 1367 (s), 1390 (m) cm⁻¹. ¹³C NMR (CD₂Cl₂): δ = 59.31 (N-CH₂-CH₂-CH₂-CH₃), 31.43 [SiOC(CH₃)₃], 24.37 (N-CH₂-CH₂-CH₂-CH₃), 20.32 (N-CH₂-CH₂-CH₂-CH₃), 13.89 (N-CH₂-CH₂-CH₂-CH₃) ppm. ²⁹Si NMR (0.06 M, CH₂Cl₂/CD₂Cl₂): δ = -100.7 ppm. ¹⁸³W NMR (0.05 M, CH₂Cl₂/CD₂Cl₂): δ = 27.7 (J_{W-W} = 9 Hz, 4 W, W_{eq}), 75.9 (J_{W-W} = 9 Hz, 1 W, W_{ax}) ppm.

(*n*Bu₄N)₂[NbW₅O₁₉SiPh₃] (5): To a mixture of (*n*Bu₄N)₄[(NbW₅O₁₈)₂O] (1 g, 0.28 mmol) and (C₆H₅)₃SiOH (0.155 g, 0.56 mmol) was added with stirring 30 mL of dry acetonitrile. The resulting slightly cloudy solution was stirred vigorously at room temperature for 48 h under a static argon atmosphere. This solution was centrifuged for 15 min and then diethyl ether was added to the supernatant from which a white powder was precipitated under vigorous stirring. It was washed twice with diethyl ether and dried under vacuum to give 745 mg of air- and moisture-stable microcrystalline white powder, in 64% yield. C₅₀H₈₇N₂NbO₁₉SiW₅ (2060.23): calcd. C 29.12, H 4.25, N 1.36, Si 1.36, Nb 4.5, W 44.64; found C 29.15, H 4.26, N 1.32, Si 1.65, Nb 3.48, W 43.65. IR (1450–400): $\tilde{\nu}$ = 445 (vs), 504 (m), 517 (m), 552 (w), 584 (m), 703 (m), 710 (m), 787 (vs), 810 (vs), 879 (w), 951 (m), 971 (vs), 1002 (sh), 1030 (w), 1066 (w), 1106 (sh), 1117 (s), 1162 (w), 1190 (w), 1262 (w), 1430 (m) cm⁻¹. ¹H NMR (CD₂Cl₂): δ = 3.42 (t, 16 H, N-CH₂-CH₂-CH₂-CH₃), 1.8 (q, 16 H, N-CH₂-CH₂-CH₂-CH₃), 1.45 (m, 16 H, N-CH₂-CH₂-CH₂-CH₃), 1 (t, 24 H, N-CH₂-CH₂-CH₂-CH₃), 7.46 (m, 6 H, *meta*), 7.5 (dd, 3 H, *para*), 7.75 (dd, 6 H, *ortho*) ppm. ¹³C NMR (CD₂Cl₂): δ = 137.5, 142.3, 141.6, 135.2 (Ph), 59.1 (N-CH₂-CH₂-CH₂-CH₃), 24.24 (N-CH₂-CH₂-CH₂-CH₃), 20.09 (N-CH₂-CH₂-CH₂-CH₃), 13.66 (N-CH₂-CH₂-CH₂-CH₃) ppm. ²⁹Si NMR (0.06 M, CH₂Cl₂/CD₂Cl₂): δ = -12.8 ppm. ¹⁸³W NMR (0.04 M, CH₂Cl₂/CD₂Cl₂): δ = 30.7 (J_{W-W} = 8.7 Hz, 4 W, W_{eq}), 79.0 (J_{W-W} = 9.2 Hz, 1 W, W_{ax}) ppm. The product is contaminated by a very small amount of hexatungstate W₆O₁₉²⁻ as shown by ¹⁸³W NMR spectroscopy.

Acknowledgments

This work is supported by the Centre National de Recherche Scientifique (CNRS), France and the Direction Générale de la Recherche Scientifique (DGRST), Tunisia in the frame of a bilateral joint project. We gratefully acknowledge the Comité Mixte pour la Coopération Universitaire (CMCU) (program 05G1211). We are also grateful to Patrick Herson (UPMC) for crystal data collection and for his assistance in structure resolution, and to Jocelyne Maquet for her help in recording the ²⁹Si solid-state CP-MAS spectra on the Bruker Avance 400 spectrometer (S.I.A.R.E. UPMC).

- [1] M. T. Pope, *Heteropoly and Isopoly Oxometalates*, Springer Verlag, Heidelberg, Germany, **1983**.
- [2] P. Gouzerh, A. Proust, *Chem. Rev.* **1998**, 98, 77 and references cited therein.
- [3] V. W. Day, W. G. Klemperer, *Science* **1985**, 228, 533.
- [4] D. A. Robert, G. L. Geoffrey in *Comprehensive Organometallic Chemistry* (Eds.: G. Wilkinson, F. G. A. Stone, E. W. Abel), Pergamon, Oxford, **1982**, chapter 40.
- [5] W. A. Nugent, J. M. Mayer, *Metal-Ligand Multiple Bonds*, Wiley, New York, **1988**, p. 28 and chapter 6.
- [6] B. O. West, *Polyhedron* **1989**, 8, 219.
- [7] E. V. Radkov, V. G. Young, R. H. Beer, *J. Am. Chem. Soc.* **1999**, 121, 8953.
- [8] Y. J. Lu, R. Lalancette, R. H. Beer, *Inorg. Chem.* **1996**, 35, 2524–2529.
- [9] R. G. Finke, M. W. Droegge, *J. Am. Chem. Soc.* **1984**, 106, 7274.
- [10] D. J. Edlund, R. J. Saxton, D. K. Lyon, R. G. Finke, *Organometallics* **1988**, 7, 1692.
- [11] R. G. Finke, K. Nomiya, C. A. Green, M. W. Droegge, *Inorg. Synth.* **1992**, 29, 239.
- [12] F. Bannani, H. Driss, R. Thouvenot, M. Debbabi, *J. Chem. Crystallogr.* **2007**, 37, 37.
- [13] G. M. Sheldrick, *SHELXS86*, program for the solution of crystal structure, University of Göttingen, Germany, **1986**.
- [14] D. J. Watkin, C. K. Prout, J. R. Carruthers, P. W. Betteridge, R. I. Cooper, *CRYSTALS*, Chemical Crystallography Laboratory, University of Oxford, **2001**.
- [15] K. Brandenburg, *DIAMOND*, version 2.0, Gerhard-Domagk-Straße 1, 53121 Bonn, Germany, **1998**.
- [16] L. J. Pearce, D. J. Watkin, *CAMERON*, Chemical Crystallography Laboratory, University of Oxford, **1996**.
- [17] P. J. Hay, W. R. Wadt, *J. Chem. Phys.* **1985**, 82, 270.
- [18] J. M. Maestre, J. P. Sarasa, C. Bo, J. M. Poblet, *Inorg. Chem.* **1998**, 37, 3071–3077.
- [19] C. J. Besecker, W. G. Klemperer, D. J. Maltbie, D. A. Wright, *Inorg. Chem.* **1985**, 24, 1027.
- [20] E. V. Radkov, Y. J. Lu, R. H. Beer, *Inorg. Chem.* **2000**, 39, 191–198.
- [21] V. W. Day, W. G. Klemperer, C. Schwartz, *J. Am. Chem. Soc.* **1987**, 109, 6030–6034.
- [22] A. Mazeaud, N. Ammari, F. Robert, R. Thouvenot, *Angew. Chem. Int. Ed. Engl.* **1996**, 35, 1961.
- [23] C. Rocchiccioli-Deltcheff, R. Thouvenot, M. Dabbabi, *Spectrochim. Acta, Ser. A* **1977**, 33, 143.
- [24] N. Ammari, G. Hervé, R. Thouvenot, *New J. Chem.* **1991**, 15, 607.
- [25] C. R. Mayer, R. Thouvenot, *J. Chem. Soc. Dalton Trans.* **1998**, 7–13.
- [26] C. R. Mayer, I. Fournier, R. Thouvenot, *Eur. J. Inorg. Chem.* **2000**, 6, 205.
- [27] D. Agustin, J. Dallery, C. Coelho, A. Proust, R. Thouvenot, *J. Organomet. Chem.* **2007**, 692, 746.
- [28] E. Cadot, R. Thouvenot, A. Tézé, G. Hervé, *Inorg. Chem.* **1992**, 31, 4128–4133.
- [29] J. Fuchs, W. Freiwald, H. Hartl, *Acta Crystallogr., Sect. B* **1987**, 34, 1764.

Received: March 30, 2007
Published Online: July 24, 2007